Contents lists available at SciOpen

Food Science and Human Wellness

journal homepage: https://www.sciopen.com/journal/2097-0765

China Food Publishing Co.

Gardeniae Fructus oil alleviate depression-like behaviors *via* the microbiota-gut-brain axis in mice with chronic unpredictable mild stress

Man Han[1], Fei Zeng[1], Yi Liu, Wenxin Shi, Shijuan Shao, Chunchao Yan*, Yunzhong Chen*

Hubei Provincial Research Center for TCM Health Food Engineering, Hubei Shizhen Laboratory, Hubei University of Chinese Medicine, Wuhan 430065, China

ARTICLE INFO

Article history:
Received 12 June 2024
Received in revised form 31 July 2024
Accepted 5 September 2024

Keywords:
Gardeniae Fructus oil
Chemical composition
Depression
Gut microbiota
TLR4/NF-κB/NLRP3 pathway
Fecal microbiota transplantation

ABSTRACT

Depression poses a considerable threat to global health, underscoring the critical need for safe treatments. Because of its homology of medicine and food, Gardeniae Fructus is widely used in clinical and everyday life contexts. Gardeniae Fructus oil (OGF) is a waste byproduct of the food industry with promising recycling potential. While previous research has demonstrated the antidepressant effects of OGF, the precise mechanism remains unclear. To fill this gap in the literature, this paper elucidates the composition and potential antidepressant mechanism of OGF. According to the results, OGF is mainly composed of fatty acids and unsaponifiable matter. OGF could effectively attenuate depression-like behaviors in mice with chronic unpredictable mild stress by modulating the microbiota-gut-brain axis. Mechanisms include improving gut dysbiosis, regulating short-chain fatty acids, protecting the intestinal barrier function, reducing hippocampal damage, and alleviating neuroinflammation by inhibiting the activation of the TLR4/NF-κB/NLRP3 pathway. Fecal microbiota transplantation experiments confirmed the involvement of the gut microbiota in the modulation of depression-like behavior by OGF. This study establishes the antidepressant effects of OGF as well as the underlying mechanism, demonstrating its potential as a novel dietary intervention for depression treatment.

1. Introduction

Depression, a prevalent mental illness, is anticipated to become the top global burden of disease by 2030. The World Health Organization reported that depression affects more than 300 million people worldwide, contributing to nearly 800 000 suicides annually[1]. In 2020, the COVID-19 pandemic has exacerbated depression and anxiety rates by 25%[2]. Currently, pharmacological therapy, particularly selective serotonin reuptake inhibitors such as fluoxetine, remains the primary treatment for depression[3]. However, because of the severity of the side effects of these antidepressants, more effective and safer alternatives from botanic resources need to be urgently found. Indeed, oils derived from natural plants have been reported to alleviate depression-like symptoms by modulating the gut microbiome[4-5].

Gardeniae Fructus, the desiccated mature fruit of *Gardenia jasminoides* Ellis, is not only a natural medicinal plant with dysphoria relieving effect, but also a traditional food in China. Currently, natural additives extracted from Gardeniae Fructus are widely used in the food industry. However, after their extraction, the remaining Gardeniae Fructus oil (OGF) is not effectively utilized. Furthermore, it has been proven that OGF has the potential to rapidly improve depression-like behaviors. In a previous study, unmodeled normal mice were used, which were only gavaged with a high OGF dose for one day before assessing effects[6]. However, the antidepressant effect of OGF on depressed individuals as well as the precise mechanism remain unclear.

[1] These authors contributed equally to this work.
* Corresponding authors at: Hubei University of Chinese Medicine, Wuhan 430065, China.
E-mail address: chyzh6204@126.com (Y.Z. Chen); mophey@126.com (C.C. Yan)
Peer review under responsibility of Beijing Academy of Food Sciences.

Publishing services by Tsinghua University Press

http://doi.org/10.26599/FSHW.2024.9250403

The microbiota-gut-brain (MGB) axis plays a pivotal role in the onset and progression of depression, highlighting it as a promising therapeutic target[7]. Gut microbiota actively participate in the bidirectional communication between the gastrointestinal tract and the central nervous system, thereby influencing immune-inflammatory responses, neurotransmitters, and metabolites. For example, a previous study demonstrated that the transferal of fecal microbiota from the feces of depressed humans to healthy rats could induce both depressive behaviors and physiological changes in the latter; both clinical and animal studies evidenced that fecal microbiota transplantation (FMT) can ameliorate depressive symptoms[8]. This suggests that behavioral and physiological aspects of depression can be reproduced through gut microbial transfer.

In the present study, OGF was hypothesized to improve depression-like symptoms in a mouse model for chronic unpredictable mild stress (CUMS) by regulating the MGB axis. Therefore, the fatty acid and unsaponifiable matter in OGF were firstly analyzed through gas chromatography-mass spectrometry (GC-MS) to infer effective components. Furthermore, the antidepressant efficacy of OGF was assessed using a CUMS-induced mouse model. In addition, the potential mechanisms underlying the antidepressant effect of OGF were explored based on the MGB axis; its effects on the intestinal barrier, gut microbiota, hippocampus, related signaling pathways, and FMT were assessed.

2. Materials and methods

2.1 Materials

Gardeniae Fructus (Batch No.: 20220101) was obtained from Hubei Qiangkang Traditional Chinese Medicine Slices Co., Ltd. (Ezhou, China). OGF was obtained by petroleum ether extraction of Gardeniae Fructus for 3 times. Fluoxetine hydrochloride dispersible tablets (Batch No.: 21518A) were obtained from Patheon France. Primary antibodies against β-actin (GB15003), occludin (GB111401), Toll-like receptor 4 (TLR4, GB11519), NOD-like receptor thermal protein domain associated protein 3 (NLRP3, GB114320), apoptosis-associated speck-like protein containing a CARD (ASC, GB113966), and interleukin-1β (IL-1β, GB11113) as well as the secondary antibody (GB23303) were obtained from Servicebio Technology Co., Ltd. (Wuhan, China). Primary antibodies against zonula occludens-1 (ZO-1; AF5145) and cleaved Caspase-1 (AF4005) were obtained from Affinity Biosciences (Changzhou, China). Primary antibodies against claudin-1 (13050-1-AP) and nuclear factor kappa-B (NF-κB, 80979-1-RR) were obtained from Proteintech Biotechnology Co., Ltd. (Wuhan, China). The primary antibody against p-NF-κB (WL02169) was obtained from Wanleibio Co., Ltd. (Shenyang, China).

2.2 Chemical analysis of OGF

2.2.1 Analysis of fatty acids

OGF samples were subjected to saponification of fats and methyl esterification of fatty acids according to a previous study[9]. Samples were then analyzed using GC-MS (Trace 1600/ISQ 7610, Thermo Fisher, USA). The following chromatographic conditions were set: Thermo TR-FAME column (100 m × 0.25 mm, 0.20 μm); injection volume, 1 μL; split ratio, 10:1. The initial programmed temperature of 60 °C was maintained for 5 min, then increased to 160 °C at 5 °C/min, and finally increased to 240 °C at 2 °C/min, which was maintained for 15 min.

2.2.2 Analysis of unsaponifiable matter

OGF samples were subjected to the extraction of unsaponifiable matter according to a previous study[10]. Samples were then analyzed using GC-MS (AI 1310/Trace 1300/ISQ QD, Thermo Fisher, USA). The following chromatographic conditions were set: Thermo TG-5MS column (30 m × 0.25 mm, 0.25 μm); injection volume, 1 μL; split ratio, 5:1. The initial programmed temperature of 60 °C was maintained for 1 min, then increased to 240 °C at 10 °C/min, which was maintained for 1 min, and further increased to 280 °C at 2 °C/min, which was maintained for 1 min; finally, the temperature was further increased to 295 °C at 1 °C/min, which was maintained for 1 min.

2.3 CUMS

2.3.1 Animals

A total of 72 male ICR mice (4 weeks old, 21–23 g) were obtained from Hunan SJA Laboratory Animal Co., Ltd. (Changsha, China) under license number SCXK (Xiang) 2019-0004. All animal procedures were approved by the Animal Ethics Committee of Wuhan Myhalic Biotechnology Co. (Approval No. HLK-20230413-001). During the entire study, all mice were housed under an ambient temperature of (22 ± 2) °C, relative humidity of (55 ± 5)%, and a 12-h light/dark cycle. Mice received a standard diet and water *ad libitum*.

2.3.2 Establishment of depression model and experimental design

Mice were kept in individual cages and exposed to the CUMS program for 6 weeks[11]. Each mouse randomly received 1 long-term and 1 short-term stressor, and the same stressors were not used for 2 consecutive days. This protocol included the following stressors: 8 long-term stressors (for 24 h) such as fasting, water deprivation, white noise (90 dB), stroboscopic light source, odor stimulation, 45° cage tilting, empty cage, and wet bedding; 6 short-term stressors such as restraint (6 h), swimming in cold water (4 °C for 5 min), heat stress in an oven (55 °C for 10 min), cage shaking (2 h), tail pinching (2 min), and electrical stimulation (0.6 mA, 50 s). The specific daily schedule of long-term and short-term stressors is shown in Table S1.

After an adaptation period of 1 week, the mice were randomly allocated to 6 groups (n = 12): Control group (CON), CUMS + Solvent group (CUMS), CUMS + Fluoxetine 3.03 mg/kg group (FLU), CUMS + OGF 61 mg/kg group (OGF-L), CUMS + OGF 122 mg/kg group (OGF-M), and CUMS + OGF 244 mg/kg group (OGF-H). The recommended clinical dosage of fluoxetine was 20 mg/60 kg·day and the equivalent dosage for mice converted by their body surface area was 3.03 mg/kg. The recommended clinical dosage of Gardeniae Fructus was 10 g/60 kg·day and the medium OGF dosage for mice converted by their body surface area and the extraction rate of OGF was 122 mg/kg.

Except for the CON group that had 6 mice per cage, each mouse of the remaining 5 groups was housed in a separate cage. During the 6-week CUMS program, mice were treated with a 4-week drug regimen starting in the third week. Moreover, mice received treatment at a fixed time each morning, and the modeling procedure was performed 1 h after drug administration. All drugs were prepared with 0.5% Tween 80 as solvent and were administered by gavage. Finally, behavioral tests were performed for 1 week.

2.4 Body weight and food intake

To evaluate the effects of both the CUMS program and administered drugs on the physical condition of mice, the body weight and food intake were calculated for each mouse. During the experimental period, the body weight of each mouse was recorded weekly and food intake was noted every 2 weeks.

2.5 Behavioral tests

2.5.1 Sucrose preference test (SPT)

The SPT is commonly used to assess the degree of anhedonia by observing sucrose consumption, which is considered as a core symptom of depression[12]. The SPT was performed every 2 weeks during the experiment: during the adaptation period (week 0), before drug treatment (week 2), during drug treatment (week 4), and before animal sacrifice (week 6).

Firstly, all mice were trained to acclimatize to one bottle of 1% sucrose water and one bottle of pure water for 48 h and the positions of both bottles were exchanged every 12 h. Then, mice were deprived of water for 24 h. Subsequently, each mouse was given a bottle with 60 mL pure water and a bottle with 60 mL 1% sucrose solution for 24 h, where the positions of both bottles were also switched after 12 h. The consumed amounts of sucrose solution and pure water were recorded by weighing the bottles before and after the test. Sucrose preference was calculated according to the following formula:

$$\text{Sucrose preference (\%)} = \frac{\text{Sucrose intake (g)}}{\text{Water intake (g)} + \text{Sucrose intake (g)}} \times 100 \quad (1)$$

2.5.2 Novelty-suppressed feeding test (NSFT)

The NSFT is widely used to evaluate behavioral indicators of depression and anxiety[13]. The test was conducted over 2 days: on the 1st day, mice were placed individually in a white open box for 10 min to adapt and were fasted for 24 h. On the 2nd day, 2–3 food pills were placed in the center of the open box, and then, mice were slowly placed in the corner of the box. The test lasted for 5 min and the feeding latency period was recorded, which was the time from the start of the test until the mice could be heard gnawing. After each test, the open box was cleaned with 75% ethanol to prevent leftover odors from affecting the next test.

2.5.3 Forced swimming test (FST)

The FST was developed to assess the degree of behavioral desperation of animals in distress[14]. Mice were placed alone into a glass cylinder (height: 25 cm, diameter: 12 cm) containing water ((25 ± 1) °C, at a depth of 15 cm) and were forced to swim for 6 min. The total immobility time in the last 5 min was analyzed by SuperFst 3.0 (NJKEWBIO, Nanjing, China). Mice were considered immobile when they floated in water without struggling or when they moved only slightly to keep their heads above the surface. Between tests, glass cylinders were cleaned, and the water inside was replaced.

2.5.4 Tail suspension test (TST)

The TST was developed to assess the degree of desperation of animals under adversity[15]. Mice were secured with tape 1 cm from the tip of the tail and kept suspended from the test apparatus for 6 min. After 1 min of acclimatization, the immobility time of each mouse was measured during the last 5 min by SuperTst 3.0 (NJKEWBIO). Mice were considered immobile when they hung passively without struggling.

2.5.5 Open field test (OFT)

The OFT was used to evaluate the autonomous motor ability, exploratory behavior, and anxiety state of animals[14]. Mice were gently placed in the center of an open field box (50 cm × 50 cm × 40 cm) and allowed to explore the inside freely for 5 min. At the same time, the activity behavior was tracked by a video camera and further analyzed by KEMaze 3.3 (NJKEWBIO) to obtain relevant parameters, including the total distance traveled and the time spent in the center area. The center area was defined as the 4 squares in the middle of the box, when the bottom of the box was divided into 16 equally sized squares.

2.5.6 Elevated plus-maze (EPM) test

The EPM test was used to examine the anxiety state of mice[16], using an apparatus consisting of a central platform and 4 mutually perpendicular arms (5 cm × 30 cm). Two opposite arms were surrounded on three sides by 20-cm-high walls (closed arm), while the other 2 opposite arms were surrounded by no obstacles (open arm). A mouse was gently placed in the center of this maze in an orientation facing the open arm and was allowed to freely access all 4 arms for 5 min. Open-arm time was calculated according to the following formula:

$$\text{Open-arm time (\%)} = \frac{\text{Open arm time}}{\text{Total arm time}} \times 100 \quad (2)$$

2.6 Sample collection

During the last week of the CUMS procedure, fresh feces from the CON, CUMS, and OGF-M groups were collected and stored at −80 °C for preparation of fecal bacterial suspension. After behavioral tests, mice were fasted for 12 h. After anesthetizing mice with 5% isoflurane, their blood was collected and centrifuged (4 °C, 1 000 × *g*, 15 min), and serum was stored at −80 °C for later testing. Subsequently, hippocampus, colon, and cecal contents were collected, frozen in liquid nitrogen, and stored at −80 °C. In addition, portions of brain and colon were collected and fixed in 4% paraformaldehyde.

2.7 Enzyme-linked immunosorbent assay (ELISA) analysis

ELISA was performed according to the instructions provided by the ELISA kit (Bioswamp Life Science, Wuhan, China). IL-1β (MU30369), IL-6 (MU30044), TNF-α (MU30044), brain-derived neurotrophic factor (BDNF; MU30097), lipopolysaccharide (LPS; MU30451), and diamine oxidase (DAO; MU30134) were analyzed. Concentrations of IL-1β, IL-6, TNF-α, BDNF, LPS, and DAO in sera were calculated from standard curves and dilutions.

2.8 Histopathological examination

Brain and colon tissues of mice were fixed in 4% paraformaldehyde solution. Subsequently, tissues were embedded in paraffin wax and sectioned for hematoxylin-eosin (HE) staining. The CA1 and CA3 regions of hippocampus and colon were visualized using a microscope, and the depth of the colonic crypt was measured.

2.9 Western blotting analysis

Hippocampal or colon tissues were homogenized in lysis buffer and centrifuged at 12 000 × *g* for 5 min, after which, the supernatant was collected. The protein concentration of the supernatant was determined by BCA kit (Servicebio). Equal amounts of protein were separated by 6%–10% SDS-PAGE and transferred to PVDF membranes (0.45 μm). After being blocked with 5% skimmed milk at room temperature for 2 h, the membranes were incubated overnight at 4 °C with primary antibody. Primary antibodies included *β*-actin (1:10 000), ZO-1 (1:3 000), claudin-1 (1:5 000), occludin (1:5 000), TLR4 (1: 5 000), NF-κB (1:3 000), p-NF-κB (1:1 500), NLRP3 (1:3 000), ASC (1:5 000), cleaved Caspase-1 (1:1 000), and IL-1β (1:5 000). The next day, the membrane was washed 6 times with TBST for 5 min each time, and then incubated with secondary antibody (1:10 000) at room temperature for 1 h. Protein bands were captured using enhanced chemiluminescence solution on a Tanon-5200 chemiluminescent imaging system (Tanon, Shanghai, China). The optical densities of bands were analyzed by ImageJ software (version 1.54g; NIH, Bethesda, MD, USA) and normalized to *β*-actin to quantify other protein levels.

2.10 16S rRNA gene sequencing and bioinformatics analysis

DNA extraction and 16S rRNA gene sequencing for cecal contents from CON, CUMS, and OGF-M groups were conducted following a previously described method[17]. Both the V3−V4 hypervariable region of bacterial 16S rRNA gene were amplified. Deep sequencing was performed on an Illumina Novaseq 6000 platform by Allwegene Technology Co., Ltd. (Beijing, China). The *α*-diversity index and *β*-diversity distance matrix were calculated using QIIME (v1.8.0) software. Plots were drawn using R (v3.6.0) software. Permutational multivariate analysis of variance (PERMANOVA) was used to assess differences in *β*-diversity. Metastats analysis was used to compare taxonomic changes at the phylum and genus levels of microbiota between different groups. Linear discriminant analysis effect size (LEfSe) analysis was conducted using Python (v2.7) software, and the threshold of linear discriminant analysis (LDA) score was 3. PICRUSt2 analysis was conducted to predict the metabolic functions of microbiota, obtain relevant pathway information, and calculate the abundance of each functional category, using false-discovery-rate-corrected *P*-values.

2.11 Short-chain fatty acid (SCFA) concentration analysis

The concentrations of SCFAs including acetic acid, propionic acid, butyric acid, valeric acid, isobutyric acid, isovaleric acid, and hexanoic acid) in cecum contents were analyzed by 5977B GC/MSD (Agilent, USA) and DB-FFAP capillary column (30 m × 250 μm, 0.25 μm) as previously described[17]. The sample was resuspended in phosphoric acid (50 μL, 20%). In addition, 4-methylvaleric acid at a final concentration of 500 μmol/L was added as internal standard. The mixture was shaken and mixed for 2 min, centrifuged at 14 000 × *g* for 20 min, and finally, the supernatant was added to an injection bottle. The injection volume was 1 μL, and the split ratio was 10:1. The temperature programming used an initial temperature of 90 °C, which was increased to 160 °C at 10 °C/min, then to 240 °C at 40 °C/min, which was maintained for 5 min.

2.12 FMT analysis

For the preparation of the fecal bacterial suspension, the fresh feces obtained as described in section 2.6 were immediately added to pre-cooled PBS (100 mg feces per 1 mL of buffer) and vortexed for 2 min. After centrifugation at 800 × *g* for 5 min, the obtained supernatant was mixed with 30% glycerol-PBS solution in equal volumes and stored at −80 °C until transplantation[18].

A total of 24 mice were randomly assigned to 3 groups (n = 8): FMT-CON group, FMT-CUMS group, and FMT-OGF group, which meant that the mice in these 3 groups received fecal bacterial suspensions from the CON, CUMS, and OGF groups, respectively. All mice received 7-day antibiotic treatment according to previously described methods[19]. Mice were given antibiotic cocktails daily consisting of vancomycin hydrochloride (50 mg/kg), neomycin sulfate (100 mg/kg), and metronidazole (100 mg/kg). Amphotericin-B (1 mg/kg) was added to the cocktail during the first 3 days. Ampicillin sodium (1 mg/mL) was provided in drinking water[20]. After elimination of resident bacteria in the intestine, 200 μL of fecal bacterial suspension was administered to mice by gavage daily for 14 days. Subsequently, mice were subjected to behavioral tests for 1 week.

2.13 Statistical analysis

All data were analyzed using SPSS 26.0 software (IBM, Chicago, IL, USA) and are expressed as mean ± SD. All results were statistically analyzed using one-way analysis of variance (ANOVA) and significant differences were analyzed by least significant difference multiple comparisons under the assumption of equal variance. If heterogeneity of variance was detected, significant differences between groups were analyzed using one-way ANOVA and Welch tests followed by Tambane's T2 tests. $P < 0.05$ was considered to indicate statistically significant

differences. Spearman's correlation analysis was used to examine the correlation among depression-related behavioral indicators, inflammation-related indicators, BDNF, gut barrier-related indicators, gut microbiota, and SCFAs in mice.

3. Results

3.1 Chemical composition analysis of OGF

The composition of fatty acids and unsaponifiable matter in OGF was analyzed by GC-MS. The results showed that OGF consisted of 11 fatty acids (Fig. 1A and Table S2), with linoleic acid ($C_{18:2n6c}$, 46.67%), oleic acid ($C_{18:1n9c}$, 19.19%), palmitic acid ($C_{16:0}$, 17.17%), caproic acid ($C_{6:0}$, 8.31%), and α-linolenic acid ($C_{18:3n3}$, 2.67%) being the most prominent. The extraction rate of unsaponifiable matter from OGF was 3.48% (with relative standard deviation = 2.88%). A total of 43 components were identified in the unsaponifiable matter (Fig. 1B and Table S3), primarily comprising squalene (23.44%), β-sitosterol (15.75%), campesterol (9.72%), 24-methylenecycloartenol (8.05%), cycloartenol (6.4%), and stigmasterol (4.85%). The quantities of these components (squalene, campesterol, stigmasterol, and β-sitosterol) in the unsaponifiable matter of OGF were 217.75, 84.75, 43.20, and 143.76 mg/g, respectively.

3.2 The effects of OGF on body weight and food intake in CUMS-induced mice

A depressed CUMS mouse model (Fig. 2A) was established, and the weight and food intake of each mouse were regularly monitored. At the early stage of the experiment, differences in weight (Fig. 2B) and food intake (Fig. 2C) between groups were not statistically significant ($P > 0.05$). From the 2nd week of the experiment until the end, differences in weight and food intake between the CON and CUMS groups were significant ($P < 0.05$ or $P < 0.01$). Notably, OGF treatment reversed this observed trend to a certain extent.

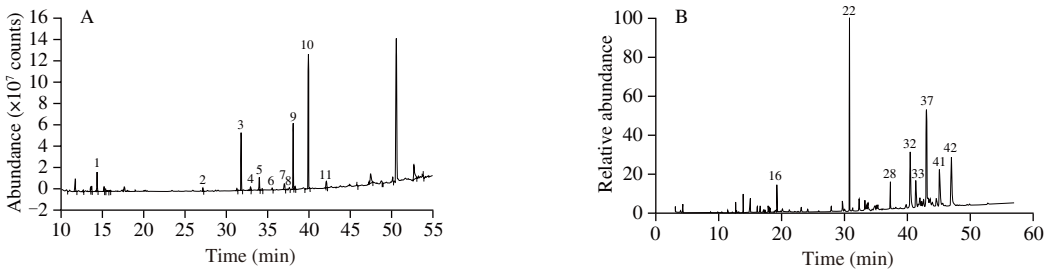

Fig. 1 Chemical composition of OGF. (A) Fatty acid compositions of OGF: (1) caproic acid, (2) myristic acid, (3) palmitic acid, (4) palmitoleic acid, (5) heptadecanoic acid, (6) *cis*-10-heptadecenoic acid, (7) stearic acid, (8) elaidic acid, (9) oleic acid, (10) linoleic acid, (11) α-linolenic acid; (B) unsaponifiable matter compositions of OGF: (16) phytol, (22) squalene, (28) hexatriacontane, (32) campesterol, (33) stigmasterol, (37) β-sitosterol, (41) cycloartenol, (42) methylenecycloartenol.

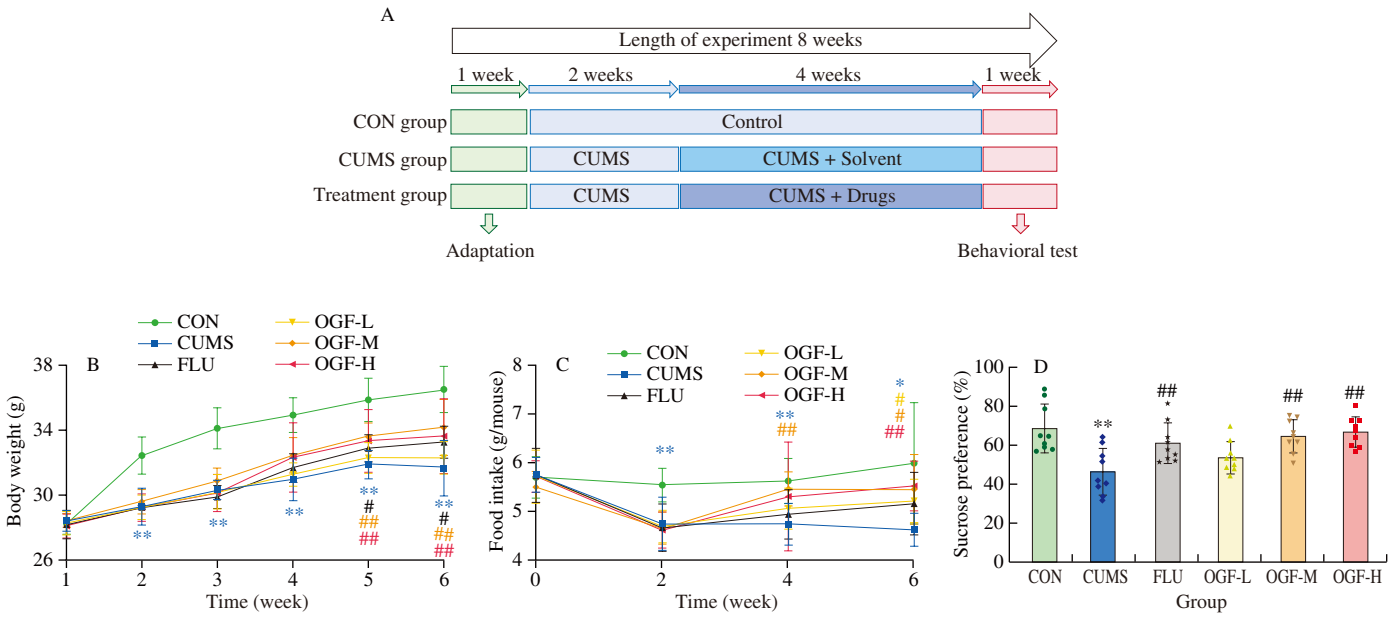

Fig. 2 Effects of OGF on depression-like behavior in CUMS-induced mice. (A) Flowchart of the experimental protocol. (B) Changes of body weight over the experiment. (C) Changes of food intake over the experiment. (D) Sucrose preference rate in the 6th week of CUMS stimulation. (E) Feeding latency in NSFT. (F) Immobility time in FST. (G) Immobility time in TST. (H) Total distance traveled in OFT. (I) Time spent in the center area in OFT. (J) Open-arm time in the EPM. (K) Motion trajectories in OFT. (L) Heat map of the motion trajectory in EPM, where the vertical axis represents the open arm and the horizontal axis represents the closed arm. Values are expressed as means ± SD (n = 9–12). *$P < 0.05$, **$P < 0.01$ *vs*. CON group; #$P < 0.05$, ##$P < 0.01$ *vs*. CUMS group. The symbols of significance in the line graph correspond to each group by color.

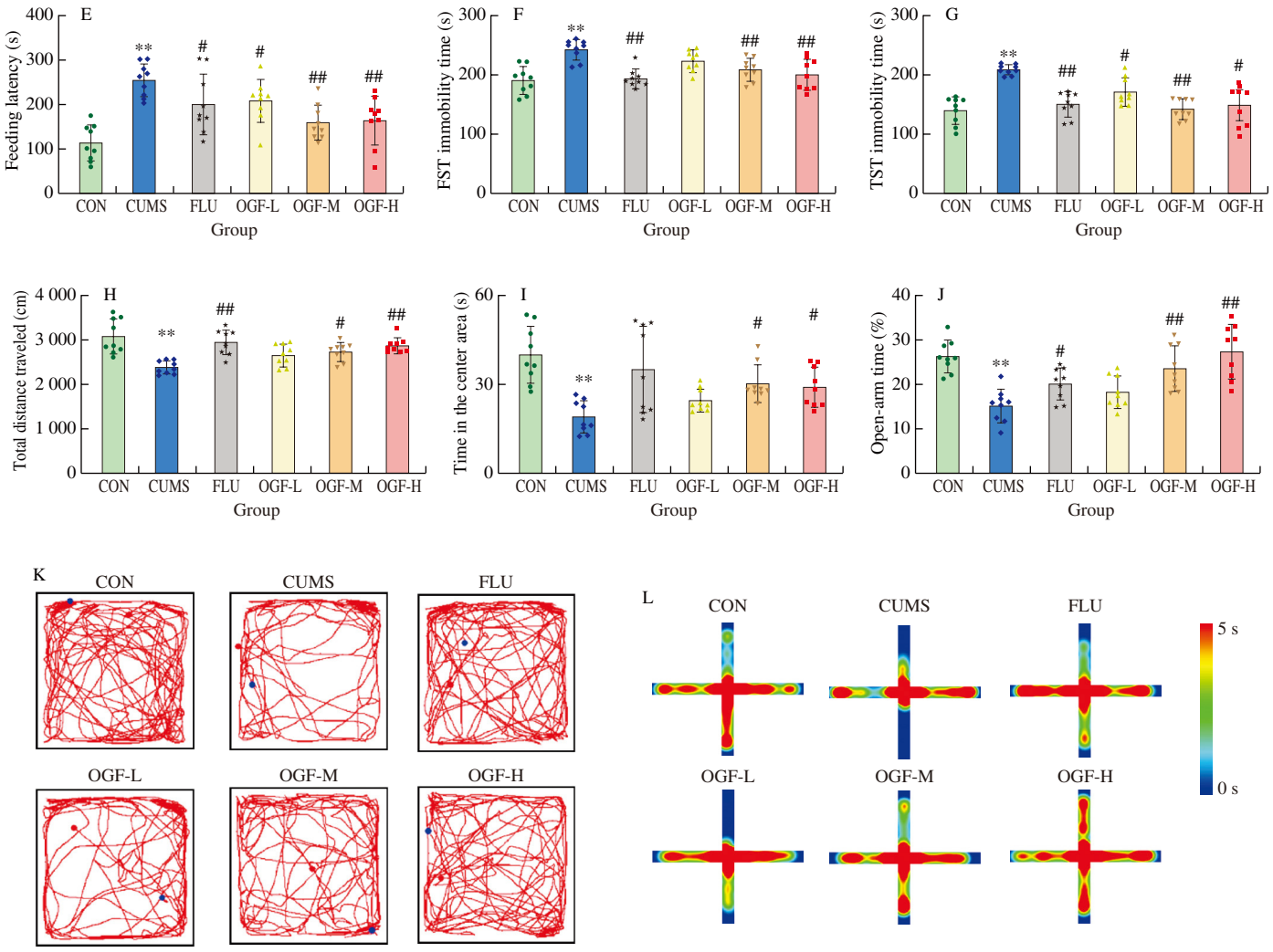

Fig. 2 (*Continued*)

3.3 OGF ameliorated depression-like behaviors in CUMS-induced mice

As shown in Figs. 2D-L and S1, CUMS-induced mice in the CUMS group exhibited great changes in anhedonia, behavioral despair, anxiety state, and exploration ability at week 6. These changes were reflected in significant reductions in sucrose preference, open-arm time, total distance traveled in OFT, and time spent in the center area of OFT compared with the CON group ($P < 0.01$); further, significant increases in feeding latency, and in immobility time of the FST, and TST were observed ($P < 0.01$). However, following treatment with fluoxetine or OGF, the above depression-like symptoms improved ($P < 0.05$ or $P < 0.01$). These results confirm that 4 weeks of OGF treatment could alleviate depressive symptoms in CUMS-induced mice.

3.4 OGF protected against hippocampal damage and modulated the level of BDNF in the serum of CUMS-induced mice

Pathological features of the hippocampus were observed using HE staining. As shown in Fig. 3A, the cerebral sections of the mice in the CON group indicated that the neuronal cells in the CA1 and CA3 regions of the hippocampus were regularly arranged, and showed normal morphology, intact structure, and clear nuclei. However, in the CUMS group, neuronal cells were reduced, and showed disorganized arrangements and enlarged cell gaps. Furthermore, a portion of cells were morphologically and structurally abnormal, with blurred outlines, pyknosis, and deeply stained nuclei. Compared with the CUMS group, the pathological damage of the hippocampus was alleviated to different degrees in all treatment groups, especially in the OGF-M and OGF-H groups. Moreover, in the CUMS group, the level of BDNF in the serum was lower than in the CON group (Fig. 3B, $P < 0.01$). However, OGF treatment increased the level of BDNF.

3.5 OGF inhibited the expression of proinflammatory cytokines in the serum of CUMS-induced mice

As depicted in Figs. 3C-E, in the CUMS group, the concentrations of IL-1β, IL-6, and TNF-α were significantly higher than in the CON group ($P < 0.01$). However, OGF and FLU treatment reduced the levels of IL-1β, IL-6, and TNF-α, suggesting that OGF could suppress the inflammatory response in CUMS-induced mice.

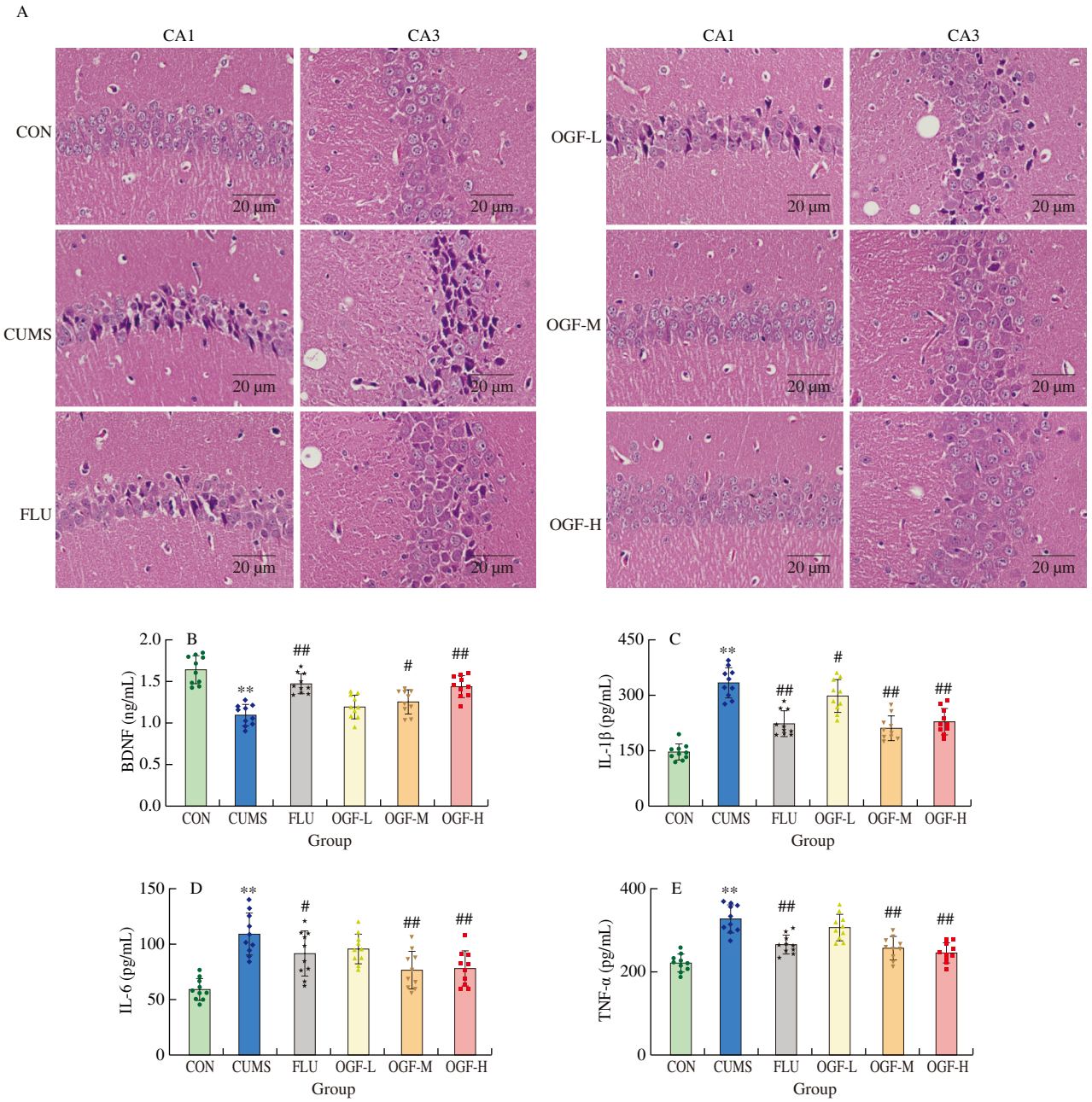

Fig. 3 Effects of OGF on hippocampal damage and the levels of BDNF and proinflammatory cytokines in CUMS-induced mice. (A) HE stained slices to observe the damage of CA1 and CA3 regions in the hippocampus. (B) BDNF. (C) IL-1β. (D) IL-6. (E) TNF-α. Values are expressed as means ± SD (n = 10). $^{**}P < 0.01$ *vs*. CON group; $^{\#}P < 0.05$, $^{\#\#}P < 0.01$ *vs*. CUMS group.

3.6 OGF protected from intestinal barrier damage caused by CUMS

Impaired intestinal barrier function may result in LPS from Gram-negative bacteria entering the circulatory system and inducing chronic inflammation[21]. Therefore, whether the CUMS program and OGF treatment altered the permeability of the intestinal barrier was examined.

Firstly, histopathological changes in the colon were observed using HE staining. As shown in Fig. 4A, in the CON group, no pathological changes in mucosal tissue damage and inflammatory cell infiltration were observed. However, in the CUMS group, colonic crypts were clearly shortened or destroyed, and inflammatory cells were infiltrated. Moreover, in the OGF group, a reduction in the inflammatory cell infiltration was observed compared with the CUMS group. The crypt depth of the colon was measured to further evaluate the effects of OGF on the intestinal barrier. In the CUMS group, the colonic crypt depth was lower than in the CON group. Importantly, in the OGF-M and OGF-H groups, this pathology was significantly reversed (Fig. 4B).

DAO, a highly active intracellular enzyme in intestinal epithelial cells, is released into the blood when the intestinal mucosal barrier is impaired. To further examine the integrity of the intestinal barrier, serum indicators of intestinal barrier function (DAO and LPS) were assayed by ELISA kits. As shown in Figs. 4C and D, stimulation by CUMS increased the levels of DAO and LPS in the serum of mice ($P < 0.01$),

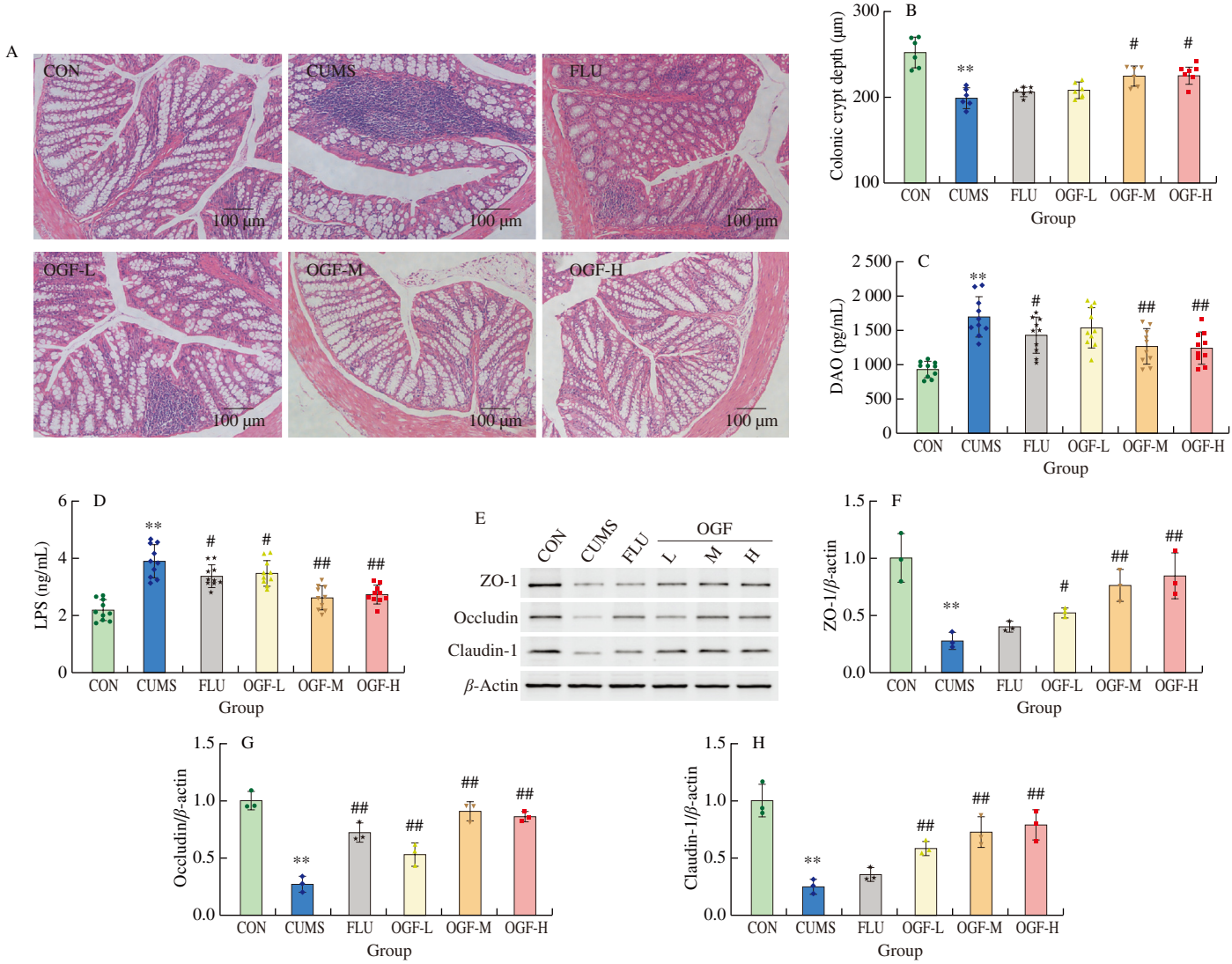

Fig. 4 Effects of OGF on the permeability of the intestinal barrier in CUMS-induced mice. (A) HE stained slices showing histopathological changes in the colon. (B) Crypt depth of the colon ($n = 5$). (C) The DAO level in serum. (D) The LPS level in serum. (E) Effects of OGF on the expression of tight junction proteins, including ZO-1 (F), occludin (G), and claudin-1 (H). The values are expressed as means ± SD ($n = 3$). $^{**}P < 0.01$ *vs*. CON group; $^{\#}P < 0.05$, $^{\#\#}P < 0.01$ *vs*. CUMS group.

while OGF treatment reduced the levels of DAO and LPS. This result suggests that OGF attenuates CUMS-induced intestinal mucosal barrier damage.

The mechanical barrier is the most important part of the intestinal mucosal barrier, and the tight junctions of intestinal epithelial cells play a key role in regulating the permeability of the intestinal mucosal barrier[22]. Therefore, Western blot analyses on the key tight junction proteins ZO-1, occludin, and claudin-1 in the colon were performed. As shown in Figs. 4E-H, the expressions of ZO-1, occludin, and claudin-1 proteins were reduced in the colon of CUMS-induced mice compared with the CON group ($P < 0.01$). Importantly, OGF treatment could reverse this downregulation of ZO-1, occludin, and claudin-1 in depressed mice ($P < 0.05$ or $P < 0.01$).

3.7 OGF affected the diversity of gut microbiota in CUMS-induced mice

The 3 experimental groups (CON, CUMS, and OGF groups) of mice shared 2 976 operational taxonomic units (OTUs), and each group had its own unique OTU (Fig. S2A). The results of construction of a Shannon-Wiener curve, a rank abundance curve, and a species accumulation curve showed that the sequencing data could reflect most of the microbial information obtained from samples (Figs. S2B-D). According to the α-diversity analysis (Table S4), no significant differences were found among the 3 groups.

More importantly, β-diversity analysis was used to examine whether OGF treatment affected the intestinal microbial community structure of mice. The weighted UniFrac distances between groups exceeded the weighted UniFrac distance within groups (Fig. 5A, $P < 0.01$), justifying the rationality of groups. The above results were also obtained in an analysis of similarities (Table S5). Moreover, OTU-based principal component analysis (PCoA) and non-metric multidimensional scaling (NMDS) analysis indicated remarkable differences in the bacterial community structure between the CUMS group and the CON group (Figs. 5B and C). Following OGF treatment, the samples of the OGF group deviated from the CUMS group and approached the CON group (PERMANOVA:CON-CUMS-OGF: $F = 2.125$, $P = 0.001$). The same results were obtained in an

analysis of molecular variance, where only CON-OGF showed no difference (Table S5, $P > 0.05$). Hence, OGF treatment could improve the structural composition of gut microbiota in CUMS-induced mice and regulate it back to the normal state.

3.8 OGF regulated the composition and function of gut microbiota in CUMS-induced mice

At the phylum level, Firmicutes, Bacteroidota, Desulfobacterota, Verrucomicrobiota, and Proteobacteria dominated samples (Fig. 5D). Compared with the CON group, the abundance of Firmicutes in the CUMS group was significantly increased (Fig. 5D, $P < 0.01$), while Bacteroidota and Spirochaetota were decreased ($P < 0.01$). Compared with the CUMS group, in the OGF group, the abundance of Firmicutes was dramatically reduced ($P < 0.01$), while that of Bacteroidota was increased ($P < 0.01$). Further, OGF treatment reversed the CUMS-induced imbalance in the Firmicutes/Bacteroidota (F/B) ratio.

At the genus level, the composition of gut microbiota for the samples of each group is shown in Fig. 5E. The relative abundances of Muribaculaceae and *Eubacterium_ventriosum*_group in the CUMS group decreased significantly, while the abundances of Lachnospiraceae_NK4A136_group, *Acetitomaculum*, and *Ruminococcus_torques*_group increased particularly compared with those in the CON group. However, OGF treatment strongly reversed the abundances of these bacteria. Furthermore, additional microbiota that exhibited decreased or increased abundance in either the CUMS or OGF group are illustrated in Figs. 5E and S3. Taken together, OGF alleviated CUMS-induced gut dysbiosis.

Gut microbiota with significant differences in abundance were obtained from CON-CUMS and CUMS-OGF by LEfSe analysis. The corresponding LDA distribution bar chart and taxonomic cladogram are shown in Figs. 6A-D. The 2 results were intersected to obtain the microflora that could regulated with OGF in the treatment of CUMS-induced mice. Among them, OGF upregulated microbiotas included c_Bacteroidia, p_Bacteroidota, o_Bacteroidales, f_Muribaculaceae, g_Muribaculaceae, g_Clostridia_vadinBB60_group, f_Clostridia_vadinBB60_group, o_Clostridia_vadinBB60_group, and s_*Alistipes_timonensis*. Down-regulated microbiotas included

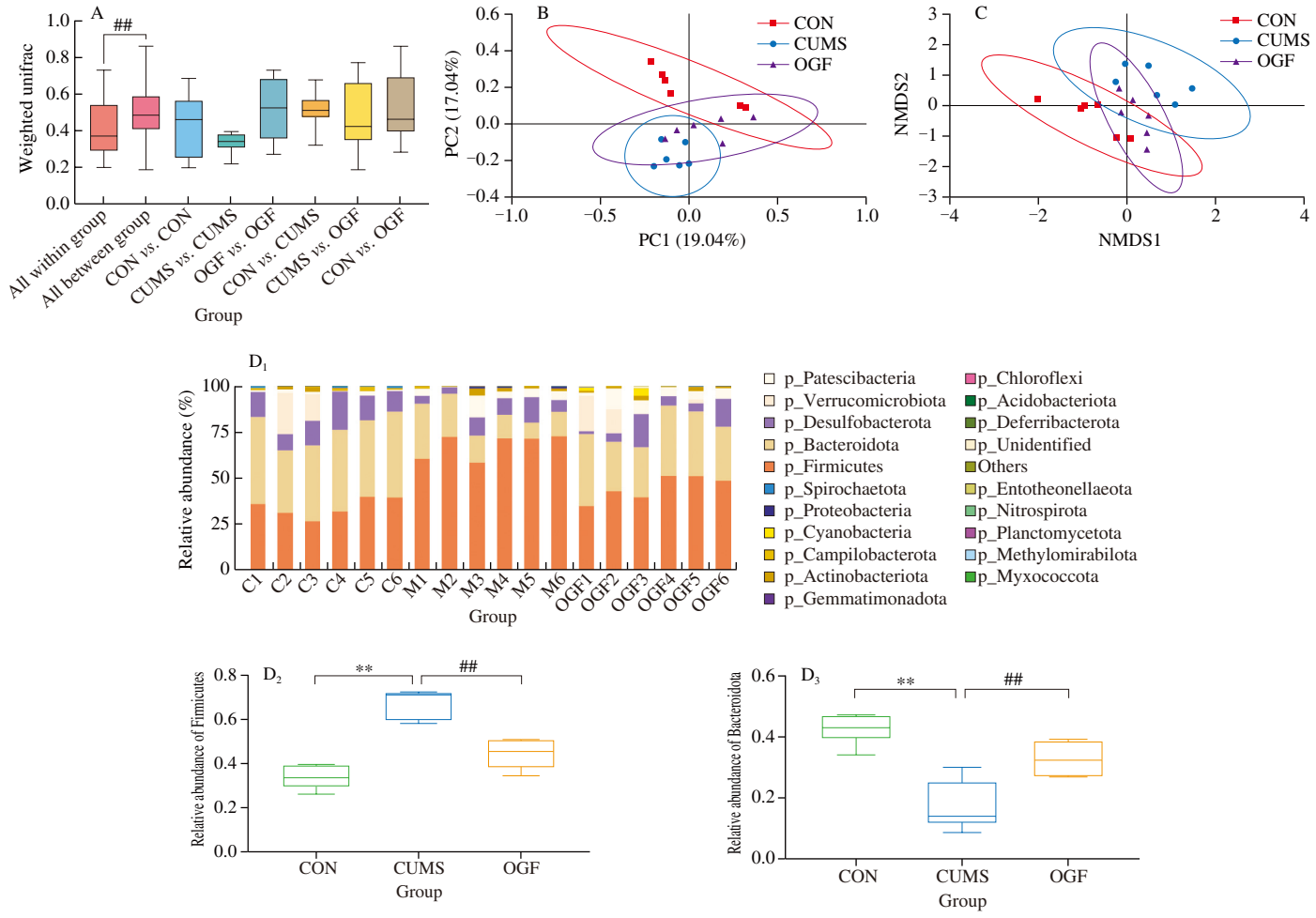

Fig. 5 Effect of OGF on β-diversity and composition of gut microbiota in CUMS-induced mice ($n = 6$). (A) Box plots of weighted UniFrac distances for samples within or between groups. (B) PCoA of the Bray-Curtis distance matrix based on OTUs. (C) NMDS analysis based on OTUs. (D) Composition and relative abundance of gut microbiota in samples from 3 groups at the phylum level. (E) Composition and relative abundance of gut microbiota in samples from 3 groups at the genus level. In the column diagram, each column represents 1 sample, and there are 18 samples in total. C, CON group; M, CUMS group; OGF, OGF group. Each column consists of differently colored blocks. Each color block and its length represent a certain microbiota and its relative abundance. Metastats analysis was used to calculate significant differences between 2 groups. $^{*}P < 0.05$, $^{**}P < 0.01$ *vs*. CON group; $^{\#}P < 0.05$, $^{\#\#}P < 0.01$ *vs*. CUMS group. n.s. no significant difference.

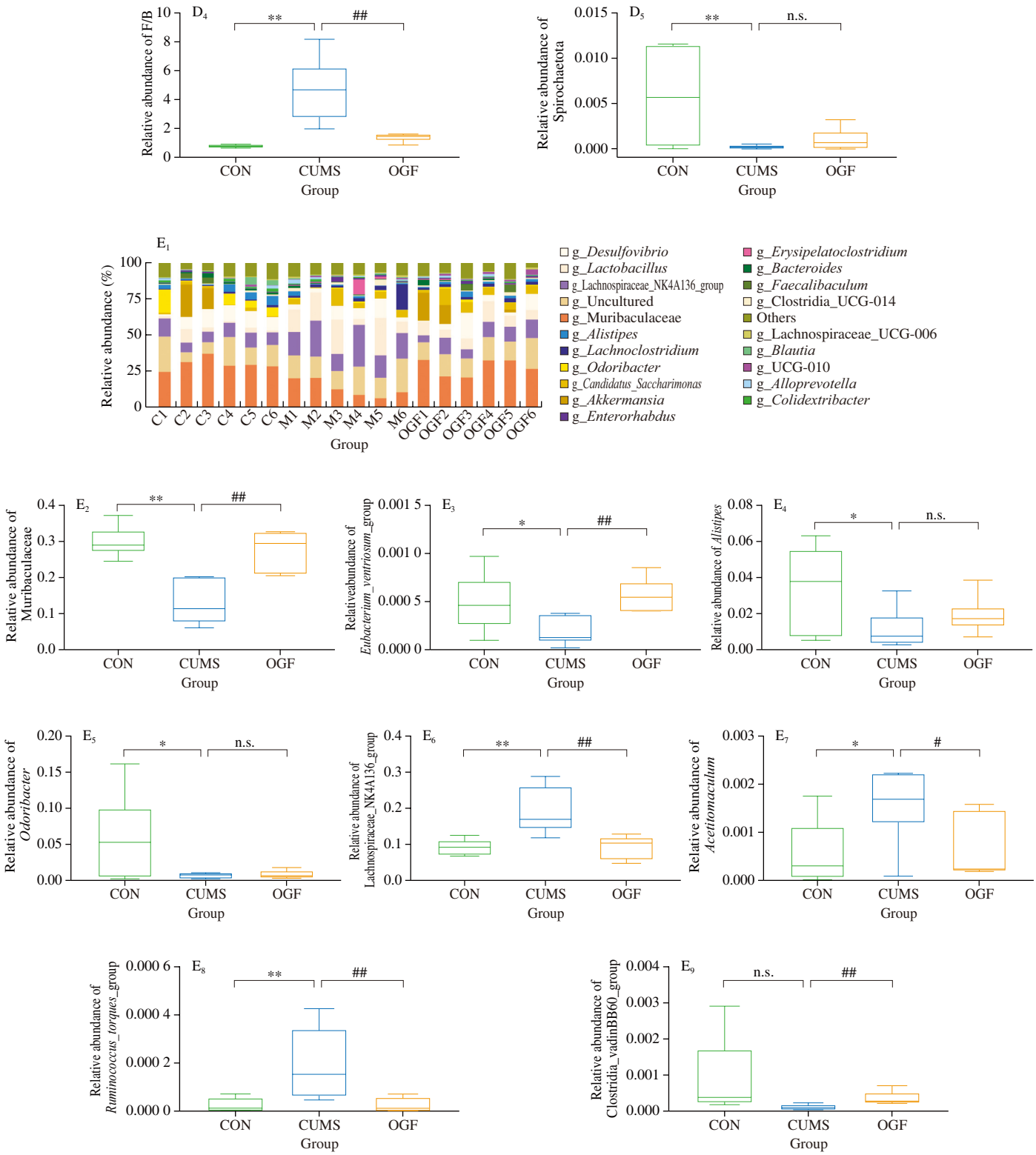

Fig. 5 (*Continued*)

p_Firmicutes, f_Lachnospiraceae, o_Lachnospirales, c_Clostridia, g_Lachnospiraceae_NK4A136_group, g_Lachnospiraceae_UCG_008, g_*Ruminococcus_torques*_group, and o_Enterobacterales. Additionally, the Kyoto Encyclopedia of Genes and Genomes (KEGG) pathways with significant differences were obtained *via* PICRUSt2 analysis among the 3 groups (Fig. 6E).

3.9 OGF recovered the level of SCFAs in the cecum of CUMS-induced mice

As the levels of SCFAs were closely related to the observed changes in gut microbiota[22], the concentrations of SCFAs were examined in the cecum contents of mice (Fig. 6F). Acetic, propionic,

Fig. 6 Effect of OGF on significantly different species, the metabolic function of gut microbiota, and the level of SCFAs in the cecal contents of CUMS-induced mice. (A) Histogram between CON and CUMS groups based on LEfSe analysis. (B) Cladogram between CON and CUMS groups based on LEfSe analysis. (C) Histogram between CUMS and OGF groups based on LEfSe analysis. (D) Cladogram between CUMS and OGF groups based on LEfSe analysis. (E) KEGG pathways with significant differences among 3 groups based on PICRUSt2 analysis. (F) Changes of SCFAs in cecal contents. In the histogram, microbiota with significant differences between groups and a LDA score exceeding 3 are shown. The length of the column reflects the LDA score, representing the effect size of microbiota with significant differences. If LDA score > 0, the microbiota is significantly upregulated in its group. In the cladogram, circles radiating from the inside to the outside represent taxonomic levels from phylum to genus. Yellow nodes represent microbiota without significant differences. Red and green nodes represent microbiota with significant differences in the corresponding groups. $^{*}P < 0.05$, $^{**}P < 0.01$ *vs*. CON group; $^{\#}P < 0.05$, $^{\#\#}P < 0.01$ *vs*. CUMS group. n.s. no significant difference.

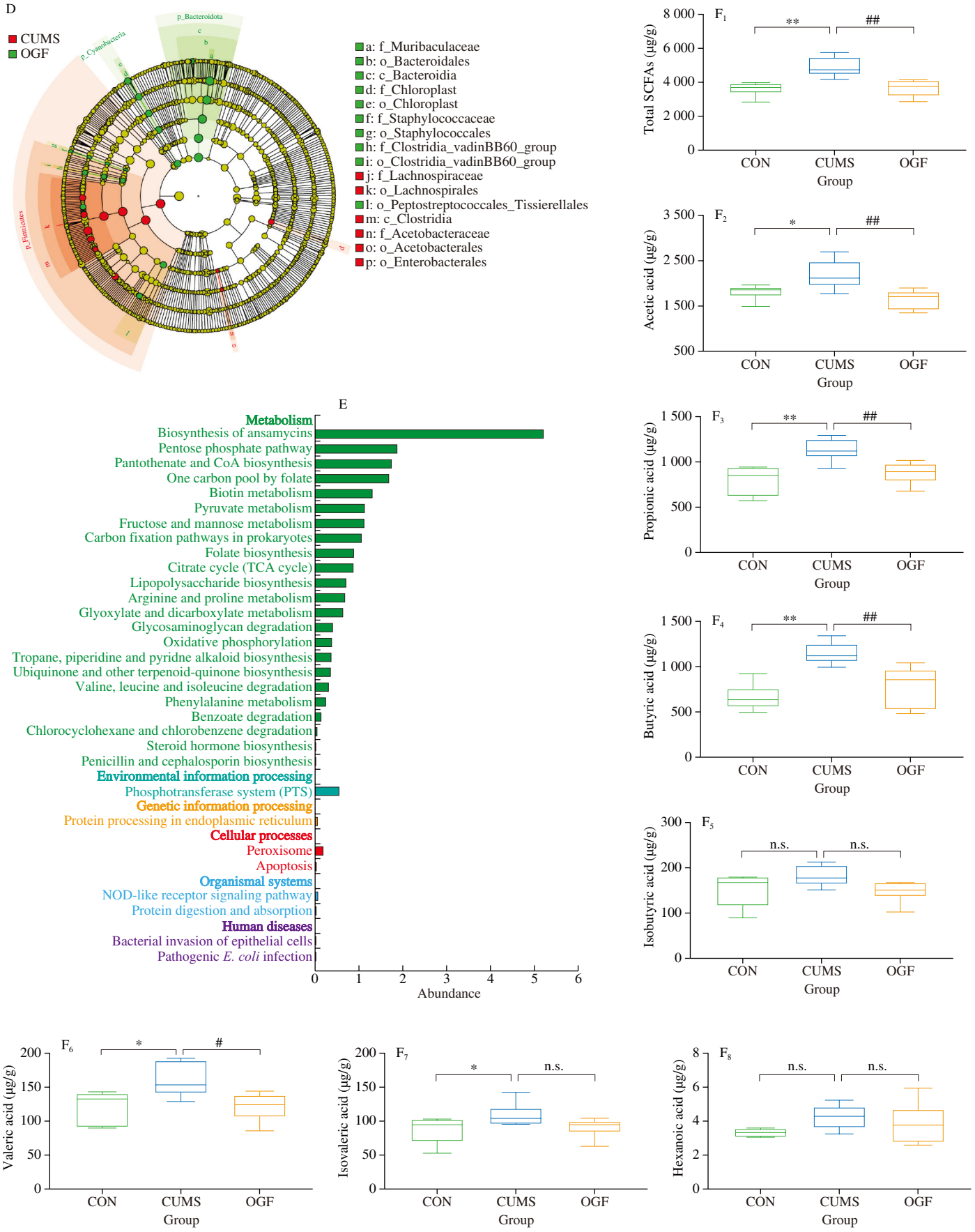

Fig. 6 (*Continued*)

and butyric acids accounted for the major components of SCFAs in cecum contents. The contents of acetic acid, propionic acid, butyric acid, and total SCFAs in the CUMS group exceeded those in the CON group ($P < 0.05$ or $P < 0.01$), while OGF treatment significantly reversed this phenomenon ($P < 0.01$). Therefore, OGF acts as an antidepressant by modulating the concentration of SCFAs.

3.10 Correlation analysis of depression-related behavioral indicators, proinflammatory cytokines, BDNF, gut barrier-related indicators, gut microbiota, and SCFAs

As shown in Fig. 7A, depression-related behavioral indicators (i.e., SPT, NSFT, FST, TST, OFT, and EPM) were significantly correlated with proinflammatory cytokines (TNF-α, IL-1β, and IL-6), BDNF, and biochemical indicators of gut barrier function (DAO and LPS). A total of 6 gut microorganisms were selected at the genus level and LEfSe difference analyses were conducted. Notably, proinflammatory cytokines (TNF-α, IL-1β, and IL-6) and gut barrier-related indicators (DAO and LPS) were negatively correlated with the abundance of Muribaculaceae and positively correlated with the abundance of Lachnospiraceae_NK4A136_group as well as the concentration of SCFAs. Conversely, BDNF had the opposite relationship with the abundance of the aforementioned microbes and the concentration of SCFAs. Consequently, OGF can be assumed to exert its antidepressant activity by altering the composition of gut microbiota, modulating SCFAs, restoring the intestinal barrier function, and attenuating inflammatory responses.

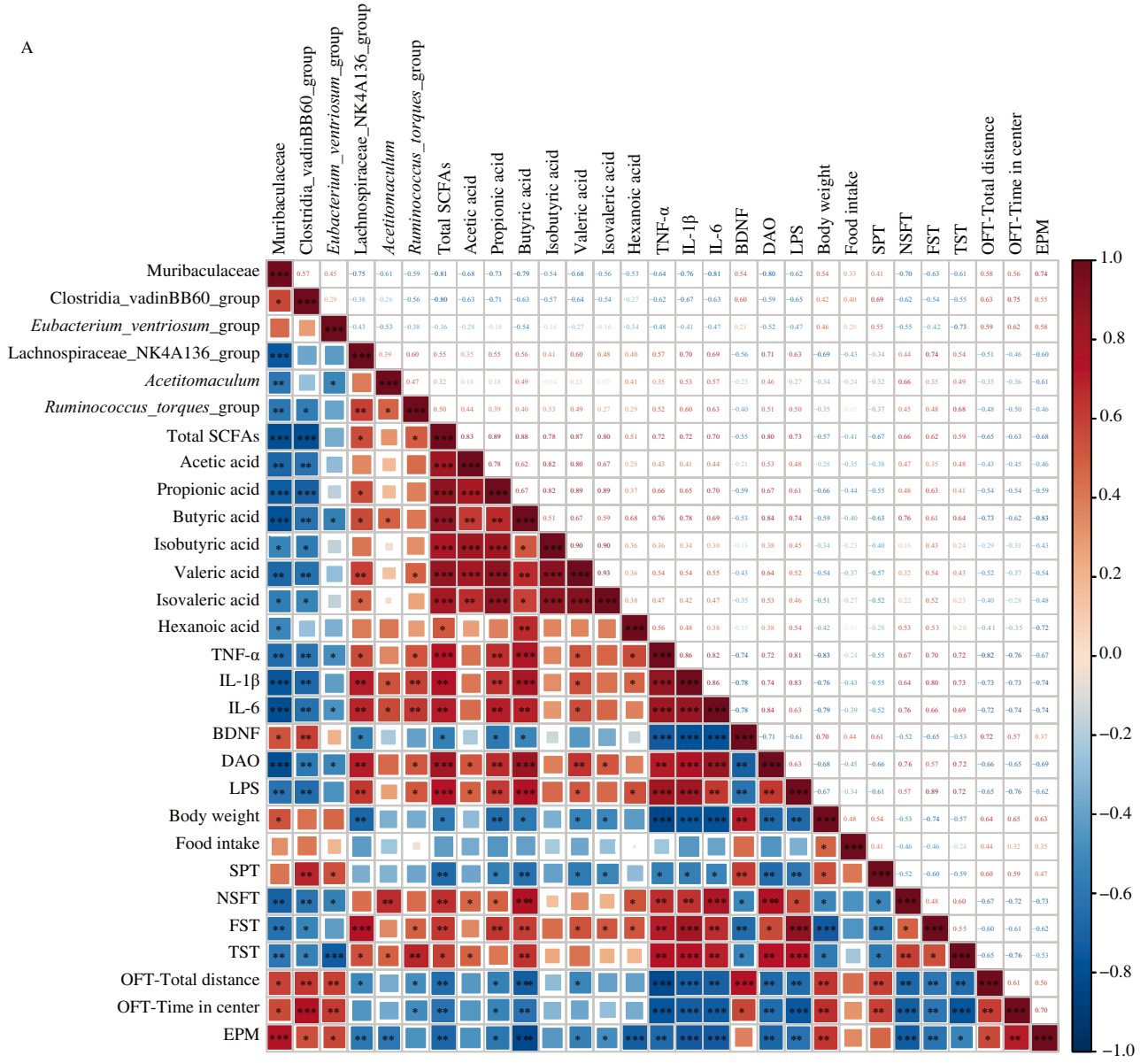

Fig. 7 Effect of OGF on correlation analysis and TLR4/NF-κB/NLRP3 pathway in CUMS-induced mice. (A) Spearman's correlation analysis of depression-related behavioral indicators, proinflammatory cytokines, BDNF, gut barrier-related indicators, gut microbiota, and SCFAs. Numbers in the upper right area represent values of correlation coefficient; symbols in the lower left area represent results of correlation and significance tests. $^{*}P < 0.05$, $^{**}P < 0.01$, $^{***}P < 0.001$. (B) Effects of OGF on the expression of proteins associated with the TLR4/NF-κB/NLRP3 signaling pathway. $^{*}P < 0.05$, $^{**}P < 0.01$ *vs*. CON group; $^{\#}P < 0.05$, $^{\#\#}P < 0.01$ *vs*. CUMS group.

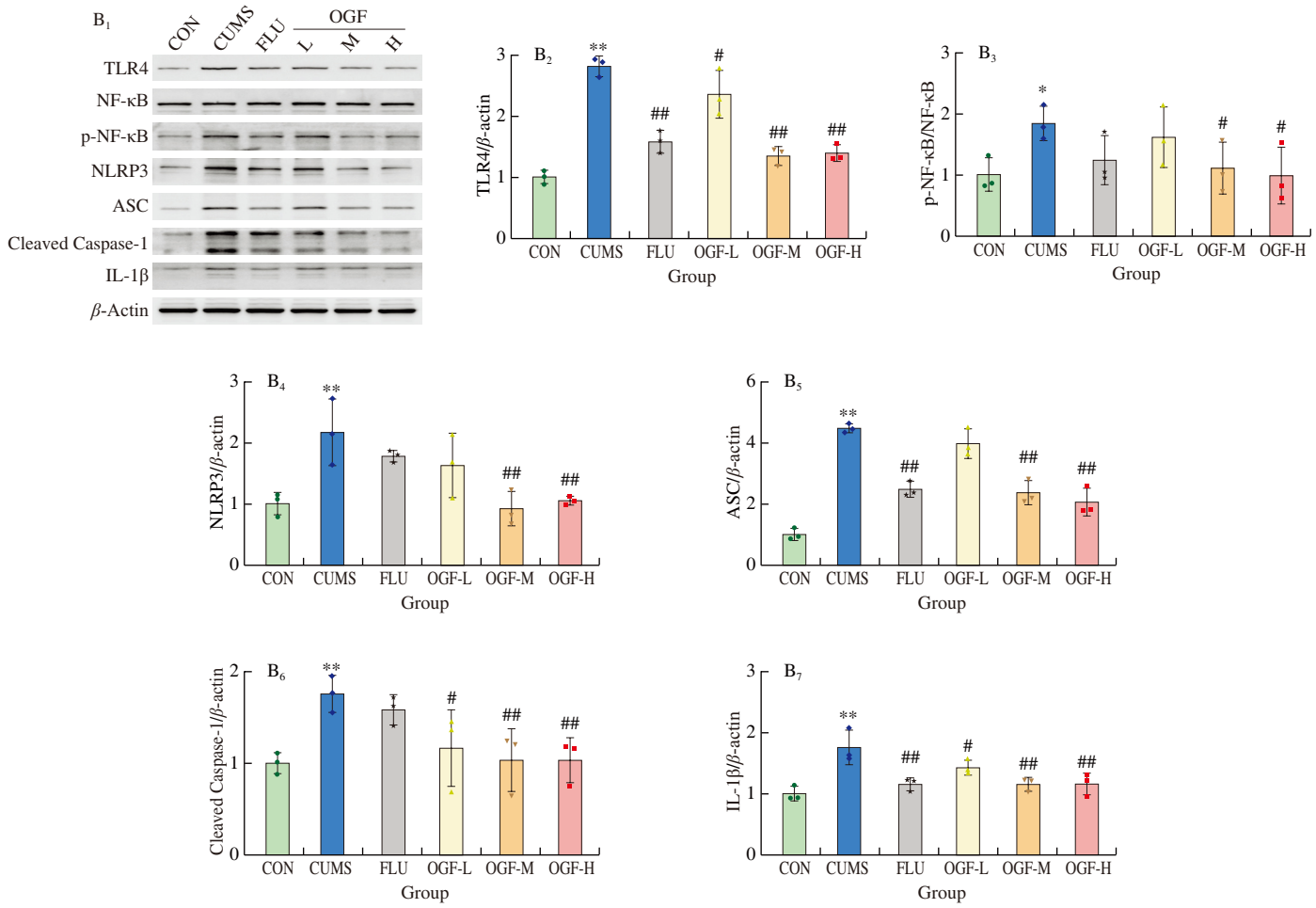

Fig. 7 (*Continued*)

3.11 OGF reversed CUMS-induced activation of the TLR4/NF-κB/NLRP3 pathway in the hippocampus of mice

Given the significant association of proinflammatory cytokines with behavioral indicators of depression and gut microbiota, the impact of OGF on the TLR4/NF-κB/NLRP3 pathway in the hippocampus of CUMS-induced mice was further examined. As shown in Fig. 7B, CUMS resulted in elevated protein levels of TLR4, p-NF-κB, NLRP3, ASC, and IL-1β, and the significant activation of Caspase-1 (P45) to cleaved Caspase-1 (P20, $P < 0.01$). Interestingly, OGF was able to reverse this observation. In addition, the changes in protein expression of IL-1β in the hippocampus corresponded to results measured in the serum.

3.12 Effects of the transplantation of CUMS or OGF microbiota on weight and depressive-like behavior in recipient mice

FMT was conducted to conform that OGF indeed improved depression in mice through gut microbiota (Fig. 8A)[23]. In comparison to recipient mice that had been colonized with CON microbiota (FMT-CON), those colonized with CUMS microbiota (FMT-CUMS)

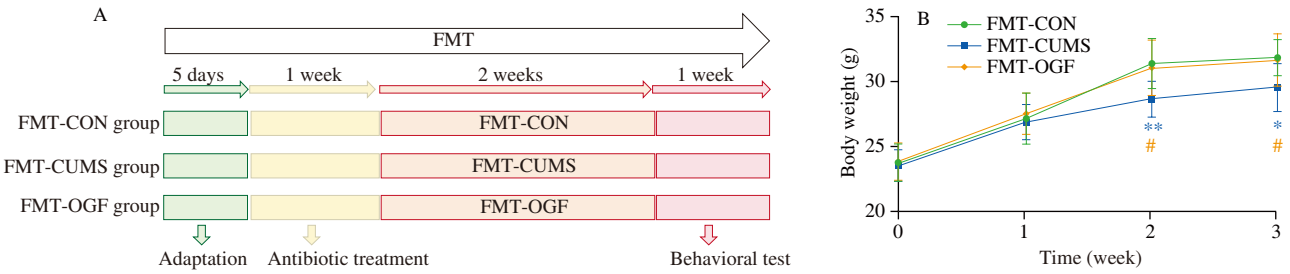

Fig. 8 Transplantation of CUMS or OGF microbiota on weight and depressive-like behaviors in the recipient mice. (A) Experimental design of FMT. (B) Changes of body weight. (C) Changes of food intake. (D) Sucrose preference rate at the end of the experiment. (E) Feeding latency in NSFT. (F) Immobility time in FST. (G) Immobility time in TST. (H) Total distance traveled in OFT. (I) Time spent in the center area in OFT. (J) Open-arm time in EPM. $^{*}P < 0.05$, $^{**}P < 0.01$ *vs*. FMT-CON group; $^{\#}P < 0.05$, $^{\#\#}P < 0.01$ *vs*. FMT-CUMS group. The symbols of significance in the line graph correspond to each group by color.

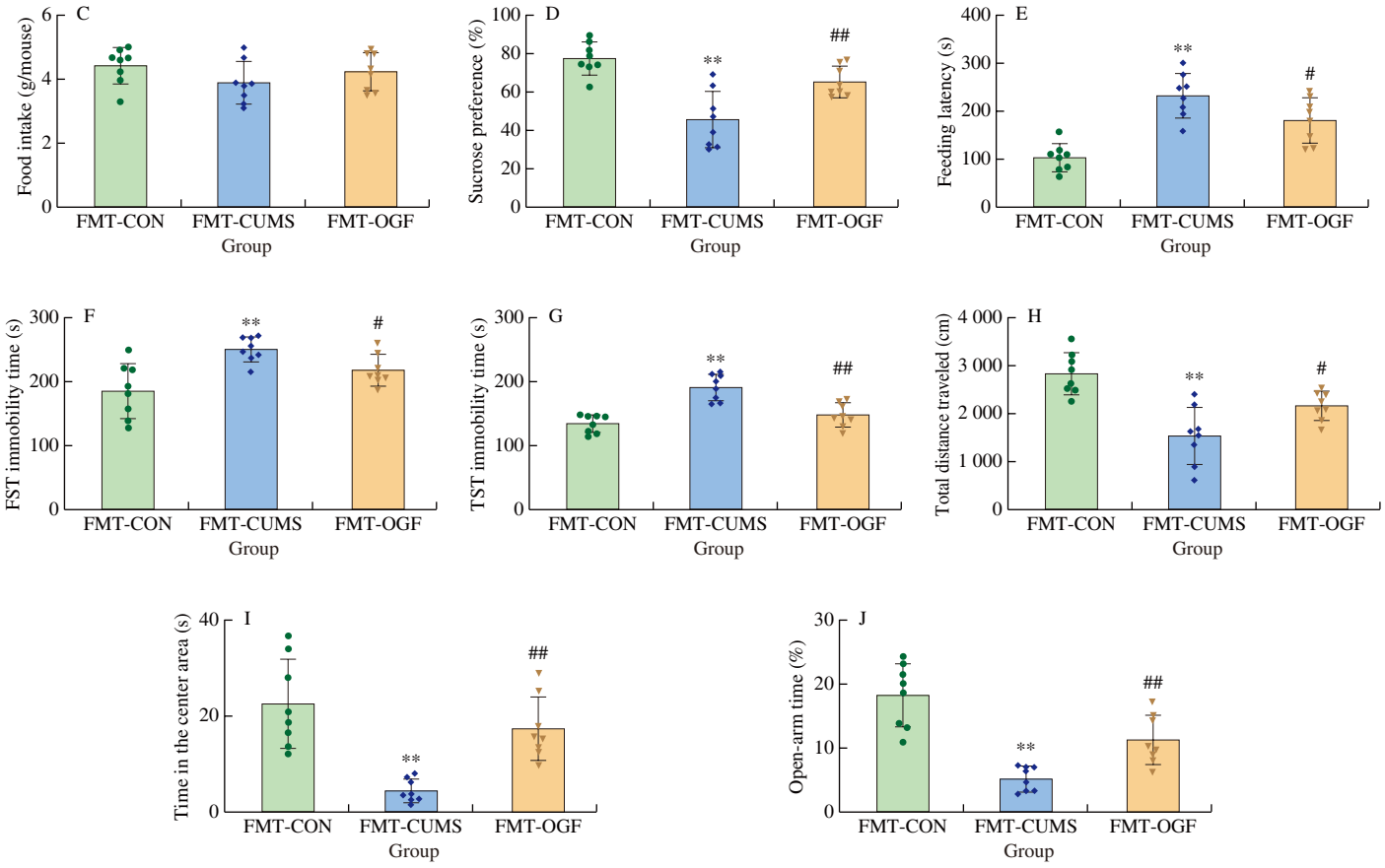

Fig. 8 (*Continued*)

showed a reduction in body weight (Fig. 8B). Conversely, mice colonized with OGF microbiota (FMT-OGF) had higher body weight than the mice of the FMT-CUMS group. In addition, no significant differences in food intake were found among all 3 groups of recipient mice (Fig. 8C). When compared with the FMT-CON group, mice in the FMT-CUMS group displayed more depressive symptoms in SPT, NSFT, FST, TST, OFT, and EPM tests (Figs. 8D-J). Notably, depressive-like behaviors were significantly ameliorated in the FMT-OGF group compared with the FMT-CUMS group.

4. Discussion

In OGF, the ratio of saturated fatty acids to monounsaturated fatty acids to polyunsaturated fatty acids is approximately 1.37:1:2.31. As essential fatty acids, polyunsaturated fatty acids in OGF mainly include linoleic acid and α-linolenic acid, which play important regulatory roles in both nervous system and cardiovascular system[24]. Especially α-linolenic acid exhibits therapeutic properties against depression, inflammation, and modulation of gut microbiota[8,25]. The monounsaturated fatty acids were dominated by oleic acid, which has various beneficial effects on the body, including protecting the neurological function of the brain, improving the mucosal barrier function of the gastrointestinal tract, and regulating gut microbiota[24]. In addition, unsaponifiable matter in OGF mainly included squalene and β-sitosterol. It has been reported that squalene exerts antidepressant effects by reducing neuroinflammation and regulating neurotransmitters[26]. β-Sitosterol is not only an antidepressant but also regulates gut barrier function and microbiota[27-28]. Preliminary research showed that crocetin in OGF also had the aforementioned effects[29]. In the present study, results from both behavioral tests and hippocampal pathology demonstrated that OGF could ameliorate CUMS-induced brain damage and depressive-like behaviors. Therefore, it was hypothesized that its antidepressant effects are closely related to these chemical components and further, that gut microbiota may be involved in this process.

Previous research confirmed the connection between depression and inflammation[30]. For instance, both social and psychological stressors can trigger excessive activation of the inflammatory system, thereby increasing vulnerability to depression. Clinical studies have identified heightened levels of pro-inflammatory cytokines (such as IL-1β, IL-6, and TNF-α) in both the brain and serum of depressed individuals compared to non-depressed individuals[31]. Additionally, interventions targeting inflammation have shown promise in ameliorating depressive symptoms. This study further showed that OGF effectively mitigated the elevation of proinflammatory cytokines in the serum of CUMS-induced mice.

The gut microbiota plays a crucial role in the bidirectional communication between the gastrointestinal system and the central nervous system by modulating immune-inflammatory responses, neurotransmitters, and various metabolites[7]. Dysbiosis in gut microbiota can disrupt intestinal integrity, consequently impacting the MGB axis, potentially leading to depression. Gut inflammation triggered by dysbiosis stimulates the release of pro-inflammatory cytokines, which compromises both the intestinal and blood-brain

barriers, ultimately leading to neuroinflammation. In the present study, compromised intestinal barrier function was observed in CUMS-induced mice, which is consistent with prior research[32]. Treatment with OGF restored colonic barrier function, suggesting its potential to exert antidepressant effects by modulating the MGB axis.

The results of β-diversity analysis indicated that OGF treatment restored the structural composition of gut microbiota of depressed mice toward a normal state. At the phylum level, OGF suppressed the increase in F/B ratio in depressed mice, aligning it with levels observed in non-depressed mice. The balance of the F/B ratio is crucial to maintain a stable gut microbiota environment. Imbalances, such as elevated F/B ratios, might trigger inflammatory responses. Notably, in children with autism spectrum disorders, a higher F/B ratio compared to normal children was observed[33].

At the genus level, 6 different microbiotas were identified using Metastats and LEfSe analyses, including Muribaculaceae, *Eubacterium_ventriosum*_group, Clostridia_vadinBB60_group, Lachnospiraceae_NK4A136_group, *Acetitomaculum*, and *Ruminococcus_torques*_group. Muribaculaceae (formerly known as S24-7) predominate the gut microbiota of mice, exhibiting the production of SCFAs and regulatory effects against harmful bacteria and inflammation[34]. In mouse models of depression and colitis, a notable decrease in the relative abundance of Muribaculaceae was reported[35]. Extensive clinical data support that *Eubacterium_ventriosum*_group diminishes with escalating depressive symptoms[36]. In the present study, a significant decrease in the abundance of *Eubacterium_ventriosum*_group compared to normal individuals was observed, which could be reversed by OGF treatment. Noteworthy, polyunsaturated fatty acids have been shown to positively regulate *Eubacterium*[37]. Lachnospiraceae_NK4A136_group and *Acetitomaculum*, both part of the Lachnospiraceae family, have been clinically linked to depression[38]. Lachnospiraceae_NK4A136_group, which is known for its production of butyric acid, plays a key role in maintaining levels of intestinal SCFAs and is considered an indicator of gut dysbiosis[39]. Moreover, its increased abundance in disease model mice (such as colitis) could be mitigated post drug treatment[40], aligning with the observations of the present study. In addition, clinical evidence has suggested increased abundance of *Ruminococcus_torques*_group associated with neurological disorders[41]. Antidepressants, such as fluoxetine, can reduce the abundance of *Ruminococcus_torques*_group[42], a response that was also observed under OGF treatment in this study. Therefore, OGF may play an antidepressant role by restoring gut dysbiosis.

SCFAs are primarily produced through the fermentation of carbohydrates by anaerobic microorganisms within the gut. SCFAs can either directly or indirectly influence communication along the brain-gut axis through various pathways, including immune, endocrine, and vagal routes[43]. In the present study, a significant increase in SCFA levels was observed in the cecal contents of depressed mice, aligning with prior research findings[44]. However, excessive levels of SCFAs have been associated with more adverse effects than benefits under certain contexts. Specifically, excesses of butyric acid and valeric acid can exacerbate colitis and autism[45], respectively. Furthermore, heightened SCFA levels in the brain-gut axis may contribute to tissue inflammation and schizophrenia[46]. Remarkably, OGF treatment effectively normalized SCFA levels in depressed mice to levels observed in healthy mice.

As mentioned above, there is a link between inflammation, gut microbiota, and depression. The results of correlation analysis showed that proinflammatory cytokines are closely related to behavioral and intestinal barrier indicators. A review of relevant literature showed that SCFAs in cecal contents and LPS in serum are associated with the downstream TLR4/NF-κB/NLRP3 signaling pathway, which could lead to neuroinflammation. TLR4 can be activated by SCFAs, thereby altering bacterial homeostasis and causing inflammation[47]. LPS is a component of the extracellular membrane of Gram-negative bacteria. With increasing permeability of the intestinal barrier, LPS permeates the circulatory system more readily and enters the brain where it induces neuroinflammation; this happens mainly through the TLR4/NF-κB pathway and activation of the NLRP3 inflammasome[48]. Specifically, LPS activates TLR4 after a series of binding, recognition, and delivery actions, which subsequently leads to NF-κB nuclear translocation and the production of inflammatory cytokines. Components of the NLRP3 inflammasome (i.e., NLRP3, ASC, and Caspase-1) are recruited and activated by various internal and external stimuli, leading to releases of IL-1β and IL-18, which further exacerbate the inflammatory response[49]. The present research demonstrated that OGF modulated the TLR4/NF-κB/NLRP3 signaling pathway in the hippocampus of mice, thereby effectively curtailing the CUMS-induced activation and mirroring previously documented outcomes[50].

FMT has been applied to treat certain psychiatric disorders in the clinic. To further confirm that OGF exerts antidepressant effects through gut microbiota, FMT was conducted. The results suggest the involvement of the gut microbiota in the regulation of weight and depressive-like behaviors.

Finally, this study is different from a previous related study[6]: In the present study, an internationally recognized CUMS depressed model was used, whereas the related previous study used normal mice. Moreover, while this study assessed the antidepressant effects of OGF in the long term, the prior study assessed it on one day only. In addition, the results of the 2 studies are also different. The result of this study focused on the MGB axis and TLR4/NF-κB/NLRP3 pathway, while the result of the prior study was limited to the PKA/CREB/BDNF pathway in the hippocampus. Interestingly, NF-κB has been shown to interact with CREB binding proteins to increase proinflammatory cytokines and neuroinflammation[51]. Therefore, in the future, more attention needs to be directed to the study of antidepressant effects of OGF and its mechanisms.

5. Conclusion

This study examined the effects of OGF on alleviating CUMS-induced depression-like behavior by modulating the MGB axis. Squalene, β-sitosterol, α-linolenic acid, and crocetin might be the main effective components of the antidepressant effect of OGF, underscoring its potential as a dietary vegetable oil. Furthermore, this regulation of OGF was achieved through the following various pathways: modulating gut microbiota, inhibiting excessive SCFAs, restoring gut barrier permeability, protecting against hippocampal damage, inhibiting the activation of the TLR4/NF-κB/NLRP3 signaling pathway, and reducing inflammation. This study provides rationales indicating that OGF could be an alternative therapy for depression, promoting the recycling of OGF as a dietary oil.

Declaration of competing interest

The authors declare that they have no known competing financial interests or personal relationships that could have appeared to influence the work reported in this paper.

Acknowledgement

This work was supported by the Natural Science Foundation of Hubei Province (2024AFD225); the Major Task Innovation Project of Hubei Province (2023BEB011); the Natural Science Foundation of Hubei Province (2023AFB403), and the Central Guided Local Science and Technology Development Special Project of Hubei Province (2019ZYYD069).

Appendix A. Supplementary data

Supplementary data associated with this article can be found, in the online version, at http://doi.org/10.26599/FSHW.2024.9250403.

References

[1] S.M. Monroe, K. L. Harkness, Major depression and its recurrences: life course matters, Annu. Rev. Clin. Psychol. 18 (2022) 329-357. https://doi.org/10.1146/annurev-clinpsy-072220-021440.

[2] H. Herrman, V. Patel, C. Kieling, et al., Time for united action on depression: a Lancet–World Psychiatric Association Commission, Lancet 399 (2022) 957-1022. https://doi.org/10.1016/S0140-6736(21)02141-3.

[3] A. Cipriani, T.A. Furukawa, G. Salanti, et al., Comparative efficacy and acceptability of 21 antidepressant drugs for the acute treatment of adults with major depressive disorder: a systematic review and network meta-analysis, Lancet 391 (2018) 1357-1366. https://doi.org/10.1016/S0140-6736(17)32802-7.

[4] C. Dang, Q. Wang, Q. Li, et al., Chinese herbal medicines for the treatment of depression: a systematic review and network meta-analysis, Front. Pharmacol. 15 (2024) 5564. https://doi.org/10.3389/fphar.2024.1295564.

[5] Y. Zhang, Y. Long, S. Yu, et al., Natural volatile oils derived from herbal medicines: a promising therapy way for treating depressive disorder, Pharmacol. Res. 164 (2021) 105376. https://doi.org/10.1016/j.phrs.2020.105376.

[6] J. Ruan, L. Liu, X. Shan, et al., Anti-depressant effects of oil from fructus gardeniae *via* PKA-CREB-BDNF signaling, Biosci. Rep. 39 (2019) BSR20190141. https://doi.org/10.1042/BSR20190141.

[7] T.G. Dinan, J.F. Cryan, Brain–gut–microbiota axis—mood, metabolism and behaviour, Nat. Rev. Gastroenterol. Hepatol. 14 (2017) 69-70. https://doi.org/10.1038/nrgastro.2016.200.

[8] S. Sonali, B. Ray, H. Ahmed Tousif, et al., Mechanistic Insights into the link between gut dysbiosis and major depression: an extensive review, Cells 11 (2022) 1362. https://doi.org/10.3390/cells11081362.

[9] P. Liu, S. Kang, Y.Y. Huang, et al., Ultrasonic-assisted extraction, fatty acids identification of the seeds oil and isolation of chemical constituent from oil residue of *Belamcanda chinensis*, Ultrason. Sonochem. 90 (2022) 106200. https://doi.org/10.1016/j.ultsonch.2022.106200.

[10] Y. Bi, G. Yang, H. Li, et al., Characterization of the chemical composition of lotus plumule oil, J. Agric. Food Chem. 54 (2006) 7672-7677. https://doi.org/10.1021/jf0607011.

[11] P. Willner, Reliability of the chronic mild stress model of depression: a user survey, Neurobiol. Stress 6 (2017) 68-77. https://doi.org/10.1016/j.ynstr.2016.08.001.

[12] J.P.H. Verharen, J.W. de Jong, Y. Zhu, et al., A computational analysis of mouse behavior in the sucrose preference test, Nat. Commun. 14 (2023) 2419. https://doi.org/10.1038/s41467-023-38028-0.

[13] J. Li, S. Tian, H. Wang, et al., Protection of hUC-MSCs against neuronal complement C3a receptor-mediated NLRP3 activation in CUMS-induced mice, Neurosci. Lett. 741 (2021) 135485. https://doi.org/10.1016/j.neulet.2020.135485.

[14] Y. Fan, Y. Bi, H. Chen, Salidroside improves chronic stress induced depressive symptoms through microglial activation suppression, Front. Pharmacol. 12 (2021) 635762. https://doi.org/10.3389/fphar.2021.635762.

[15] J.F. Cryan, C. Mombereau, A. Vassout, The tail suspension test as a model for assessing antidepressant activity: review of pharmacological and genetic studies in mice, Neurosci. Biobehav. Rev. 29 (2005) 571-625. https://doi.org/10.1016/j.neubiorev.2005.03.009.

[16] A.K. Kraeuter, P.C. Guest, Z. Sarnyai, The elevated plus maze test for measuring anxiety-like behavior in rodents, Methods Mol. Biol. 1916 (2019) 69-74. https://doi.org/10.1007/978-1-4939-8994-2_4.

[17] H. Zhou, J. Zhao, C. Liu, et al., Xanthoceraside exerts anti-Alzheimer's disease effect by remodeling gut microbiota and modulating microbial-derived metabolites level in rats, Phytomedicine 98 (2022) 153937. https://doi.org/10.1016/j.phymed.2022.153937.

[18] H. Yao, D. Zhang, H. Yu, et al., Gut microbiota regulates chronic ethanol exposure-induced depressive-like behavior through hippocampal NLRP3-mediated neuroinflammation, Mol. Psychiatry 28 (2023) 919-930. https://doi.org/10.1038/s41380-022-01841-y.

[19] C.A. Olson, H.E. Vuong, J.M. Yano, et al., The gut microbiota mediates the anti-seizure effects of the ketogenic diet, Cell 174 (2018) 497. https://doi.org/10.1016/j.cell.2018.06.051.

[20] J.M. Yano, K. Yu, G.P. Donaldson, et al., Indigenous bacteria from the gut microbiota regulate host serotonin biosynthesis, Cell 161 (2015) 264-276. https://doi.org/10.1016/j.cell.2015.02.047.

[21] Y. Mi, N. Yi, X. Xu, et al., Prebiotics alleviate cartilage degradation and inflammation in post-traumatic osteoarthritic mice by modulating the gut barrier and fecal metabolomics, Food Funct. 14 (2023) 4065-4077. https://doi.org/10.1039/D3FO00775H.

[22] C. Chelakkot, J. Ghim, S.H. Ryu, Mechanisms regulating intestinal barrier integrity and its pathological implications, Exp. Mol. Med. 50 (2018) 1-9. https://doi.org/10.1038/s12276-018-0126-x.

[23] X. Tian, G. Wang, F. Teng, et al., Zhi Zi Chi decoction (Gardeniae fructus and semen Sojae Praeparatum) attenuates anxious depression *via* modulating microbiota–gut–brain axis in corticosterone combined with chronic restraint stress-induced mice, CNS Neurosci. Ther. 30 (2024) e14519. https://doi.org/10.1111/cns.14519.

[24] D.D. Dohrmann, P. Putnik, D. Bursać Kovačević, et al., Japanese, Mediterranean and Argentinean diets and their potential roles in neurodegenerative diseases, Food Res. Int. 120 (2019) 464-477. https://doi.org/10.1016/j.foodres.2018.10.090.

[25] K.M. Appleton, P.D. Voyias, H.M. Sallis, et al., Omega-3 fatty acids for depression in adults, Cochrane Database Syst. Rev. 11 (2021) CD004692. https://doi.org/10.1002/14651858.CD004692.pub5.

[26] K. Sasaki, M.B. Othman, F. Ferdousi, et al., Modulation of the neurotransmitter systems through the anti-inflammatory and antidepressant-like effects of squalene from *Aurantiochytrium* sp, PLoS ONE 14 (2019) e0218923. https://doi.org/10.1371/journal.pone.0218923.

[27] N. Panayotis, P.A. Freund, L. Marvaldi, et al., *β*-Sitosterol reduces anxiety and synergizes with established anxiolytic drugs in mice, Cell Rep. Med. 2 (2021) 100281. https://doi.org/10.1016/j.xcrm.2021.100281.

[28] L. Ma, Y. Ma, Y. Liu, *β*-Sitosterol protects against food allergic response in BALB/c mice by regulating the intestinal barrier function and reconstructing the gut microbiota structure, Food Funct. 14 (2023) 4456-4469. https://doi.org/10.1039/D3FO00772C.

[29] S. Lin, Q. Li, S. Jiang, et al., Crocetin ameliorates chronic restraint stress-induced depression-like behaviors in mice by regulating MEK/ERK pathways and gut microbiota, J. Ethnopharmacol. 268 (2021) 113608. https://doi.org/10.1016/j.jep.2020.113608.

[30] J.K. Kiecolt-Glaser, H.M. Derry, C.P. Fagundes, Inflammation: depression fans the flames and feasts on the heat, Am. J. Psychiatry 172 (2015) 1075-1091. https://doi.org/10.1176/appi.ajp.2015.15020152.

[31] A.H. Miller, C.L. Raison, The role of inflammation in depression: from evolutionary imperative to modern treatment target, Nat. Rev. Immunol. 16 (2016) 22-34. https://doi.org/10.1038/nri.2015.5.

[32] L. Huang, Z. Ma, X. Ze, et al., Gut microbiota decreased inflammation induced by chronic unpredictable mild stress through affecting NLRP3 inflammasome, Front. Cell. Infect. Microbiol. 13 (2023) 1189008. https://doi.org/10.3389/fcimb.2023.1189008.

[33] Z. Dan, X. Mao, Q. Liu, et al., Altered gut microbial profile is associated with abnormal metabolism activity of Autism spectrum disorder, Gut Microbes 11 (2020) 1246-1267. https://doi.org/10.1080/19490976.2020.1747329.

[34] I. Lagkouvardos, T.R. Lesker, T.C.A. Hitch, et al., Sequence and cultivation study of Muribaculaceae reveals novel species, host preference, and functional potential of this yet undescribed family, Microbiome 7 (2019) 28. https://doi.org/10.1186/s40168-019-0637-2.

[35] H. He, H. He, L. Mo, et al., Priming of microglia with dysfunctional gut microbiota impairs hippocampal neurogenesis and fosters stress vulnerability of mice, Brain, Behav., Immun. 115 (2024) 280-294. https://doi.org/10.1016/j.bbi.2023.10.031.

[36] D. Radjabzadeh, J.A. Bosch, A.G. Uitterlinden, et al., Gut microbiome-wide association study of depressive symptoms, Nat. Commun. 13 (2022) 7128. https://doi.org/10.1038/s41467-022-34502-3.

[37] A. Mukherjee, C. Lordan, R.P. Ross, et al., Gut microbes from the phylogenetically diverse genus *Eubacterium* and their various contributions to gut health, Gut Microbes 12 (2020) 1802866. https://doi.org/10.1080/19490976.2020.1802866.

[38] S.G. Cheung, A.R. Goldenthal, A.C. Uhlemann, et al., Systematic review of gut microbiota and major depression, Front. Psychiatry. 10 (2019) 34. https://doi.org/10.3389/fpsyt.2019.00034.

[39] J. Liao, Y. Cao, J. Zhao, et al., Aqueous extract of *Polygala japonica* Houtt. ameliorated nonalcoholic steatohepatitis in mice through restoring the gut microbiota disorders and affecting the metabolites in feces and liver, Phytomedicine 118 (2023) 154937. https://doi.org/10.1016/j.phymed.2023.154937.

[40] J. Liu, J. Cai, P. Fan, et al., Salidroside alleviates dextran sulfate sodium-induced colitis in mice by modulating the gut microbiota, Food Funct. 14 (2023) 7506-7519. https://doi.org/10.1039/D3FO01929B.

[41] H. Nishiwaki, J. Ueyama, K. Kashihara, et al., Gut microbiota in dementia with Lewy bodies, npj Parkinson's Dis. 8 (2022) 169. https://doi.org/10.1038/s41531-022-00428-2.

[42] I. Lukić, D. Getselter, O. Ziv, et al., Antidepressants affect gut microbiota and *Ruminococcus flavefaciens* is able to abolish their effects on depressive-like behavior, Transl. Psychiatry 9 (2019) 133. https://doi.org/10.1038/s41398-019-0466-x.

[43] B. Dalile, L. Van Oudenhove, B. Vervliet, et al., The role of short-chain fatty acids in microbiota–gut–brain communication, Nat. Rev. Gastroenterol. Hepatol. 16 (2019) 461-478. https://doi.org/10.1038/s41575-019-0157-3.

[44] Y. Chen, N. Xiao, Y. Chen, et al., Semen Sojae Praeparatum alters depression-like behaviors in chronic unpredictable mild stress rats *via* intestinal microbiota, Food Res. Int. 150 (2021) 110808. https://doi.org/10.1016/j.foodres.2021.110808.

[45] S. Liu, E. Li, Z. Sun, et al., Altered gut microbiota and short chain fatty acids in Chinese children with autism spectrum disorder, Sci. Rep. 9 (2019) 287. https://doi.org/10.1038/s41598-018-36430-z.

[46] S. Ju, Y. Shin, S. Han, et al., The gut–brain axis in schizophrenia: the implications of the gut microbiome and SCFA production, Nutrients 15 (2023) 4391. https://doi.org/10.3390/nu15204391.

[47] N. Kazemian, M. Mahmoudi, F. Halperin, et al., Gut microbiota and cardiovascular disease: opportunities and challenges, Microbiome 8 (2020) 36. https://doi.org/10.1186/s40168-020-00821-0.

[48] Y. Tong, H. Fu, C. Xia, et al., Astragalin exerted antidepressant-like action through SIRT1 signaling modulated NLRP3 inflammasome deactivation, ACS Chem. Neurosci. 11 (2020) 1495-1503. https://doi.org/10.1021/acschemneuro.0c00156.

[49] K.V. Swanson, M. Deng, J.P.Y. Ting, The NLRP3 inflammasome: molecular activation and regulation to therapeutics, Nat. Rev. Immunol. 19 (2019) 477-489. https://doi.org/10.1038/s41577-019-0165-0.

[50] Y. Wang, H. Wu, S. Zhang, et al., Catalpol ameliorates depressive-like behaviors in CUMS mice *via* oxidative stress-mediated NLRP3 inflammasome and neuroinflammation, Transl. Psychiatry 11 (2021) 353. https://doi.org/10.1038/s41398-021-01468-7.

[51] J. Wang, B. Liu, F. Sun, et al., Histamine H3R antagonist counteracts the impaired hippocampal neurogenesis in lipopolysaccharide-induced neuroinflammation, Int. Immunopharmacol. 110 (2022) 109045. https://doi.org/10.1016/j.intimp.2022.109045.